



Cellulose from Renewable Materials: Isolation, Characterization and Antimicrobial Studies

T.S. KIRUTHIKA¹, E.K.T. SIVAKUMAR² and V. JAISANKAR^{1,*} 

¹PG and Research Department of Chemistry, Presidency College (Autonomous), Chennai-600005, India

²Department of Ceramic Technology, A.C. Tech, Anna University, Chennai-600025, India

*Corresponding author: E-mail: vjaisankar@gmail.com

Received: 18 May 2022;

Accepted: 8 July 2022;

Published online: 19 October 2022;

AJC-20995

The present study reported the isolation of cellulose from various plant biomass sources such as jackfruit peel, pineapple leaf, corn cob and hemp. The selected plant materials were treated with sequence of chemical and mechanical methods to remove non-cellulosic components such as lignin, pectin, holo-cellulose and hemi-cellulose. The lignin present was safely removed by treatment with peroxide and acetic acid and then isolated cellulose materials were characterized by various physico-chemical techniques. The peaks observed in the FTIR spectral analysis shows the presence of α -cellulose and absence of other biomass fractions. The morphology and average crystallinity of cellulose were examined by scanning electron microscope (SEM) and X-ray diffraction (XRD), respectively. The inhibitory effect of isolated cellulose against certain bacteria and fungi indicated good antibacterial and antifungal activities.

Keywords: Cellulose, Plant biomass, Isolation, Bionanocomposites.

INTRODUCTION

Cellulose is a polysaccharide containing D-glucose as monomeric units found in plants and non-edible parts of fruits. Every alternate glucose molecule in cellulose chains is reversed, making it an organic substance [1]. Microfibrils are formed when these chains are placed parallel to one other [2]. Green plants and algae consist of cellulose as a structural component of their major cell walls. Gram-negative bacteria species such as *Azotobacter*, *Acetobacter*, *Rhizobium*, *Pseudomonas*, *Salmonella*, Gram-positive, *Alcaligenes* bacteria species, *Acetobacter xylinum*, *Komagataeibacter hansenii* and *Acetobacter pasteurianus* are some of the bacteria that produce cellulose [3].

Cellulose constitutes the foremost renewable polymer resource offered worldwide. The quantity of cellulose in plant life species varies greatly. Never observed alone, it is usually related to many different plant substances. Wood has around half of its weight in cellulose, ranging from 40 to 50% depending on the species [4]. In flax and jute, after purification, the fibers contain natural cellulose. Grasses, ramie, cereal straws, bamboo and sugarcane (bagasse) are about to have one-third of cellulose. Since cellulose is insoluble in water, soluble only if it is separated from other constituents of plants. It is separated

from timber through a pulping technique that grinds woodchips beneath flowing water [5].

When cellulose is treated with concentrated nitric acid at elevated temperature chemically disintegrate into monomeric glucose units. Unlike starch, it possesses stiff rod-like conformation without coiling or branching [6]. Due to the presence of multiple hydroxyl groups in glucose units of cellulose, it forms hydrogen bonds with neighbouring oxygen atoms on the same or adjacent chain. This results in tightly holding of chain and forms microfibrils which are trapped in the polysaccharide matrix [7]. The distribution of the cellulose fibres throughout the lignin matrix contributes to the high tensile strength of plant stems and tree wood [8]. In this study, cellulose was isolated from plant sources such as jackfruit peel, pineapple leaves, corn cob and raw hemp. The obtained sources are washed thoroughly with water and then subjected to chemical treatments such as alkalization, delignification and bleaching. The mechanical characteristics of cellulose in primary plant cell walls are linked to plant cell development and expansion. Cellulose and its derivatives are widely used in various medical applications such as wound treatment, controlled drug delivery systems, tissue engineering, *etc.* due to their unique properties such as biocompatibility, antibacterial qualities hydrophilicity, non-toxicity and biodegradability.

This is an open access journal, and articles are distributed under the terms of the Attribution 4.0 International (CC BY 4.0) License. This license lets others distribute, remix, tweak, and build upon your work, even commercially, as long as they credit the author for the original creation. You must give appropriate credit, provide a link to the license, and indicate if changes were made.

EXPERIMENTAL

Chemicals *viz.* monochloroacetic acid, *n*-hexane, sodium hydroxide, ethanol, acetic acid, hydrogen peroxide, sodium chlorite and sodium metabisulphite. All the chemicals were purchased from Merck and used as such.

Raw materials: Hemp fibers (*Cannabis sativa* L.), jackfruit peel (*Artocarpus heterophyllus*) outer non-edible parts, pineapple leaves (*Ananas comosus*) and corn cobs (*Zea mays*) were collected from the local market. The collected samples were freed from kernels and then dried, grounded and sieved.

Fractioning of fruit biomass: A calculated quantity of each pomace (carded hemp, jackfruit non-edible part, pineapple leaf, corn cob) was washed in running water in order to remove dirt and dust. Those pomaces were dried in sunlight, meshed, sieved and weighed. About 10 g of sample is first treated with alkali solution and kept in magnetic stirrer for 3 h at 70 °C. The alkali in the fiber was removed by repeated washing with distilled water [9-12]. After alkali treatment the samples were bleached with acetate buffer (27 g of NaOH and 75 mL diluted glacial acetic acid to 1 L of distilled water) and aqueous sodium chlorite [13-16]. The slurry was washed with distilled water and then treated with dilute acetic acid [17]. Finally, pH was maintained neutral by thoroughly washed with distilled water and finally dried for 3 h. The sample obtained was white in colour shows the absence of lignin and other non-cellulosic material.

Determination of ash content: The ash content present in the isolated cellulose from plant sources was determined by taking approximately 0.5 g of vacuum dried sample. The sample was taken in dried crucible and pre-ashed in fume hood. When the smoke is ceased the sample was placed in muffle furnace at 600 °C for 6 h [18]. Then ash content of the sample was calculated using the equation below:

$$\text{Ash content} = \frac{W_i - W_o}{W} \quad (1)$$

where W_i is weight of crucible with ash, W_o is weight of the empty crucible and W is sample weight.

Determination of moisture content: The moisture content of the sample was determined by taking 0.5 g of sample in pre-weighed crucible and heating it in oven for 1 h in order to dry [19]. Then the sample with crucible was weighed. The moisture content was calculated using the equation:

$$\text{Moisture content} = \frac{W_2 - W_1}{W} \quad (2)$$

where W_1 is weight of the empty crucible, W_2 is the weight of crucible with sample and W is the weight of the sample.

Characterization: FTIR spectrum was recorded between 4000 and 400 cm^{-1} in BRUKER ALPHA-T ATR-FTIR spectrometer. The X-ray diffraction (XRD) patterns were collected from 5° to 100° in 2 θ with $\text{CuK}\alpha$ where $\lambda = 0.1542$ nm radiation on a BRUKER D8 Advance Powder X-ray diffractometer. Surface morphology of samples was examined by scanning electron microscope (HR-SEM, S2600 HITACHI). The thermal properties were analyzed using Q500 HI-RES Thermogravimetric analyzer.

RESULTS AND DISCUSSION

Isolation of cellulose: The percentage yield of cellulose obtained from the plant sources were tabulated in the Table-1. The range of yield was 67% to 90%.

TABLE-1
YIELD OBTAINED FROM DIFFERENT SOURCES

Sources (weight, g)	Yield (%)
Hemp (5 g)	90
Pineapple leaf (10 g)	72
Jackfruit peel (15 g)	70
Corn cob (10 g)	67

Compositional analysis: The compositional analysis of cellulose isolated from plant sources was carried out and the values are given in Table-2. It was observed that ash content and moisture content of the cellulose isolated from plant sources are in agreement with the reported values.

FT-IR studies: The IR spectra of cellulose extracted from hemp, pineapple leaf, jackfruit peel and corn cob material are in Fig. 1. A peak at 3380 cm^{-1} is responsible for the -OH stretching in the hemp-derived cellulose. The existence of asymmetrical stretching vibrations of -CH and -CH₂ bending caused the adsorption appeared to be at 2919 cm^{-1} [13]. A peak at 1634 cm^{-1} is due to the asymmetric stretching vibration of O-H bending, while minor intensity peaks near 1460 cm^{-1} were due to the asymmetric deformation of CH₃. The CH asymmetric deformation is represented by the peak at 1283 cm^{-1} , whereas the peak at 1132 cm^{-1} was resulted due to the -C-O-C asymmetrical stretching [17]. The ascribed peak at 878 cm^{-1} was due to CH out of plane bending of the aromatic ring, while the peak at 716 cm^{-1} was due to CH out of plane bending of the aromatic ring [11].

The cellulose prepared from pineapple leaf, the peak at 3438 cm^{-1} was caused by -OH stretching. The presence of asymmetrical stretching vibrations of -CH and -CH₂ bending was produced by 2934 cm^{-1} adsorption frequency [13]. Peaks at 1634 cm^{-1} were caused by the asymmetric stretching vibration of O-H bending, whereas smaller intensity peaks around 1428

TABLE-2
COMPOSITIONAL ANALYSIS OF CELLULOSE OBTAINED FROM VARIOUS SOURCES

Sources	Results of present study		Reported in literature survey		Ref.
	Ash content (%)	Moisture content (%)	Ash content (%)	Moisture content (%)	
Hemp	1.98 ± 0.4	5.9 ± 0.4	3.04 ± 0.1	2.6 ± 0.76	[20]
Pineapple leaf	6.2 ± 0.8	6 ± 0.6	2.19 ± 0.5	28.9 ± 0.5	[21]
Jackfruit peel	10.5 ± 0.9	15 ± 0.6	7.01 ± 0.19	12.98 ± 0.4	[12]
Corn cob	5.6 ± 0.02	6.8 ± 1.1	3.19 ± 0.01	1.6 ± 0.8	[22]

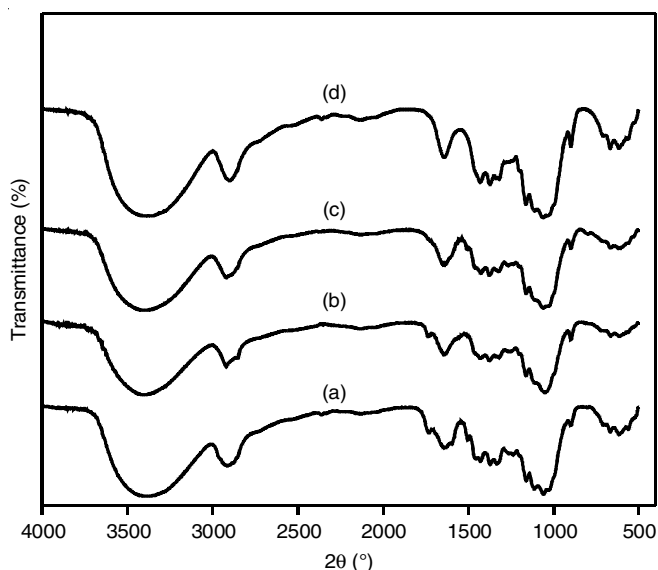


Fig. 1. FT-IR spectral studies for cellulose prepared from (a) hemp, (b) pineapple leaf, (c) jackfruit peel and (d) corn cob

cm^{-1} were caused by CH_3 asymmetric deformation. The peak at 1260 cm^{-1} represents the CH asymmetric deformation. The peak at 1160 cm^{-1} resulted in $-\text{C}-\text{O}-\text{C}$ asymmetrical stretching [17]. The assigned peak at 898 cm^{-1} was caused by the aromatic ring's CH out of plane bending, while the peak at 714 cm^{-1} was caused by the aromatic ring's CH out of plane bending.

The peak at 3424 cm^{-1} for cellulose produced from jackfruit peel was induced by $-\text{OH}$ stretching. The existence of asymmetrical stretching vibrations of $-\text{CH}$ and $-\text{CH}_2$ bending was caused by an adsorption frequency of 2923 cm^{-1} [13]. Peaks at 1641 cm^{-1} were induced by the asymmetric stretching vibration of $\text{O}-\text{H}$ bending, whereas lesser intensity peaks near 1442 cm^{-1} were caused by CH_3 asymmetric deformation. The CH asymmetric deformation is shown by the peak at 1265 cm^{-1} . The $-\text{C}-\text{O}-\text{C}$ asymmetrical stretching occurred from the peak at 1057 cm^{-1} [17]. The aromatic ring's CH out of plane bending created the assigned peak at 897 cm^{-1} , whereas the aromatic ring's CH out of plane bending caused the peak at 701 cm^{-1} .

The $-\text{OH}$ stretching generated the peak at 3420 cm^{-1} for cellulose synthesized from corn cob. An adsorption frequency of 2930 cm^{-1} induced the development of asymmetrical stretching vibrations of $-\text{CH}$ and $-\text{CH}_2$ bending [13]. Peaks at 1646 cm^{-1} were created by the asymmetric stretching vibration of $\text{O}-\text{H}$ bending, whereas peaks near 1429 cm^{-1} were caused by CH_3 asymmetric deformation. The peak at 1264 cm^{-1} represents the CH asymmetric deformation. The $-\text{C}-\text{O}-\text{C}$ asymmetrical stretching started at 1158 cm^{-1} [17]. The assigned peak at 898 cm^{-1} was generated by the aromatic ring's CH out of plane bending, whereas the assigned peak at 706 cm^{-1} was caused by the CH out of plane bending.

X-ray diffraction analysis (XRD): The X-ray diffraction spectrum for cellulose isolated from hemp, pineapple leaf, jackfruit peel and corn cob is shown in Fig. 2. On removing the non-cellulosic constituents of the samples by chemical treatment, the intensity of peak become more defined. The

presence of cellulose was verified by the presence of peaks at $2\theta = 22.8^\circ, 22.2^\circ, 22.1^\circ, 22.4^\circ$ for hemp, pineapple leaf, jackfruit peel and corn cob, respectively [23]. Among all the four sources, hemp shows the highest 2θ value and a sharp peak at 22.8° . The Scherrer's equation was used to determine the crystallite size (D) of the sample.

$$D = \frac{K\lambda}{\beta^{1/2} \cos \theta} \quad (3)$$

where λ is the wavelength of X-ray *i.e.* $\lambda = 1.54056 \text{ \AA}$, K is Scherrer's constant (0.94), $\beta^{1/2}$ is the full width half maximum (FWHM) of the peak and θ is the Bragg's angle. The crystallinity index of the dried cellulose was calculated by the following equation:

$$\text{Crystallinity index (CI)} = \frac{A_{\text{crystalline}}}{A_{\text{amorphous}} + A_{\text{crystalline}}} \times 100 \quad (4)$$

where $A_{\text{crystalline}}$ is the area of crystalline curve, $A_{\text{amorphous}}$ is the area of amorphous curve.

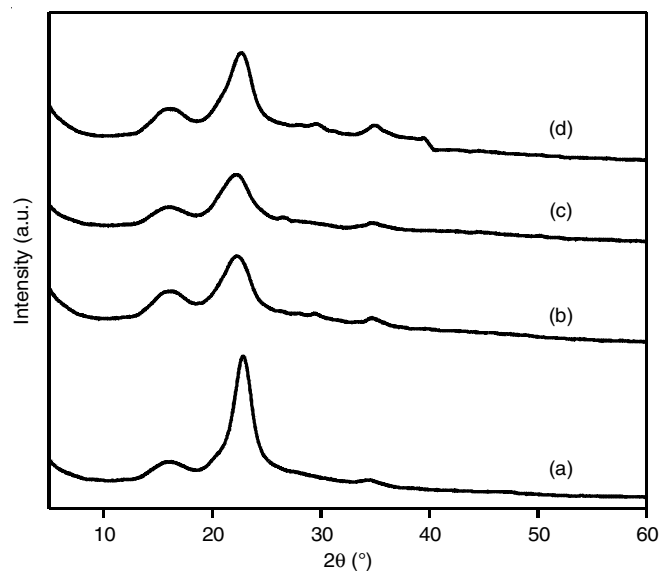


Fig. 2. XRD study of cellulose prepared from (a) hemp, (b) pineapple leaf, (c) jackfruit peel and (d) corn cob

The crystallinity index (CI) and average crystallite size (D) values of the samples are listed in Table-3. The average crystallite size value ranges from 3.58, 2.60, 4.09 and 4.08 nm for cellulose, which were isolated from hemp, pineapple leaf, corn cob and jackfruit peel, respectively [16]. The crystallite size differs according to the source of the sample. The crystallinity index (CI) and average crystalline size (D) values were increases in the order from hemp to corn cob.

TABLE-3
AVERAGE CRYSTALLITE SIZE AND
CRYSTALLINITY INDEX OF SAMPLES

Sources	Crystallinity index (%)	Average crystallite size (nm)
Hemp	47	3.58
Pineapple leaf	50	2.60
Jackfruit peel	53	4.08
Corn cob	77	4.09

TGA studies: Thermogravimetric analysis (TGA) was carried out for the cellulose isolated from hemp to study the thermal stability. The first weight loss was observed between the 25 and 96 °C is due to the moisture in the sample (Fig. 3a) [11,24]. The second weight loss occurred between 185 and 390 °C, which indicates the thermal stability of cellulose.

DTA studies: An endothermic peak at 29 and 109 °C is due to the evaporation of water molecule [11]. A sharp peak observed at 371.7 °C is occurred due to the decomposition of the cellulose [24], which confirms the presence of cellulose isolated from hemp (Fig. 3b).

SEM studies: The SEM images (Fig. 4a-h) show the fiber like morphology of the isolated cellulose prepared from hemp, pineapple leaf, corn cob and jackfruit peel. After bleaching the fibers, partial defibrillation was occurred. A reduction in the size of the individual fibers occurred because of alkali treatment and bleaching. The white colour sample indicates the removal of the non-cellulosic components such as lignin, wax, pectin and other impurities.

Antibacterial activity: The isolated cellulose from hemp were evaluated for their susceptibility against pathogenic micro-organisms by minimum inhibitory concentrations [25-28]. The antibacterial activity of hemp cellulose was determined by disc diffusion method on Muller-Hinton agar (MHA) medium [29-34]. Active cultures for experiments were prepared by transferring a loop full of culture from the stock cultures into the test tubes containing nutrient broth and then incubated at 24 h at 37 °C. After the medium was solidified, the inoculums were spread on the solid plates with sterile swab moistened with the bacterial suspension [35-38]. The disc were placed in MHA plates and added 20 µL of sample (concentration: 1000, 750 and 500 µg/mL). The plates were incubated for 24 h at 37 °C. The antimicrobial activity was determined by measuring the diameter of zone of inhibition. Table-4 shows the antibacterial activities of different bacteria on isolated cellulose. The zone of inhibition (in mm) of sample against pathogens showed a moderate to strong activity with varying concentration (500

TABLE-4
ZONE OF INHIBITION OF DIFFERENT
BACTERIA'S IN 1000, 750, 500 µg/mL

Organisms	Zone of inhibition (mm)			Antibiotic (1 mg/ mL)
	1000 µg/mL	750 µg/mL	500 µg/mL	
<i>Staphylococcus aureus</i>	7	7	7	33
<i>Pseudomonas aeruginosa</i>	7	7	7	13
<i>Enterococcus faecalis</i>	9	9	8	35
<i>Bacillus subtilis</i>	32	25	19	49
<i>Escherichia coli</i>	9	7	7	8

to 1000 µg/mL). The cellulose from hemp shows the better inhibition activity against *Bacillus subtilis*.

Antifungal activity: Minimum Inhibitory concentrations were used to test the susceptibility of hemp cellulose to the fungal activity. Antifungal activity was determined by disc diffusion method on Sabouraud Dextrose agar (SDA) medium [39-41]. Stock cultures were maintained at 4 °C on Sabouraud Dextrose agar Slant. Active cultures for experiments were prepared by transferring the stock cultures into the test tubes containing Sabouraud dextrose broth that were incubated at 48 h at room temperature. The assay was performed by agar disc diffusion method [41-43]. Sabouraud dextrose agar (SDA) medium was poured into the petriplate. After the medium was solidified, the inoculums were spread on the solid plates with sterile swab moistened with the fungal suspension. Amphotericin-B is taken as positive control. Samples and positive control of 20 µL each were added in sterile discs and placed in SDA plates. The plates were incubated for 24 h at 28 °C. Table-5 shows the zone of inhibition (in mm) of sample against pathogens showed a moderate to strong activity with varying concentration (500 to 1000 µg/mL). The cellulose from hemp shows better inhibition activity against *Dermatophyte*.

Conclusion

In this investigation, cellulose was isolated from the plant materials such as hemp, pineapple leaf, corn cob and jackfruit peel. The physico-chemical properties of the cellulose obtained

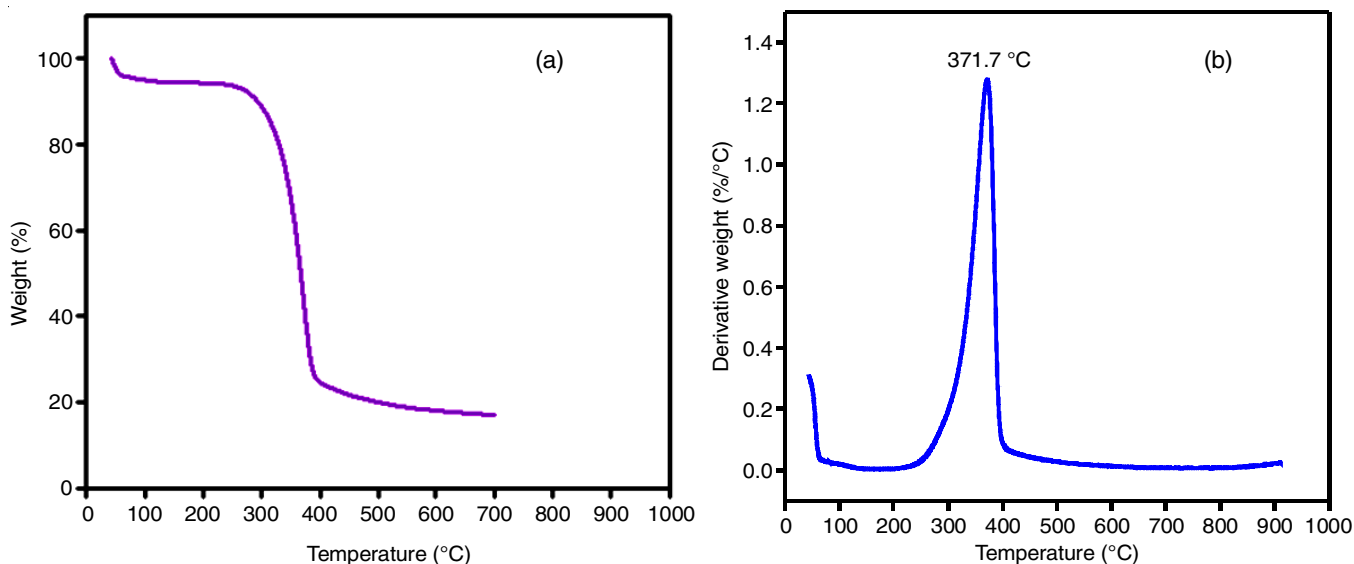


Fig. 3. (a) TGA study for cellulose from hemp, (b) DTA study for cellulose prepared from hemp

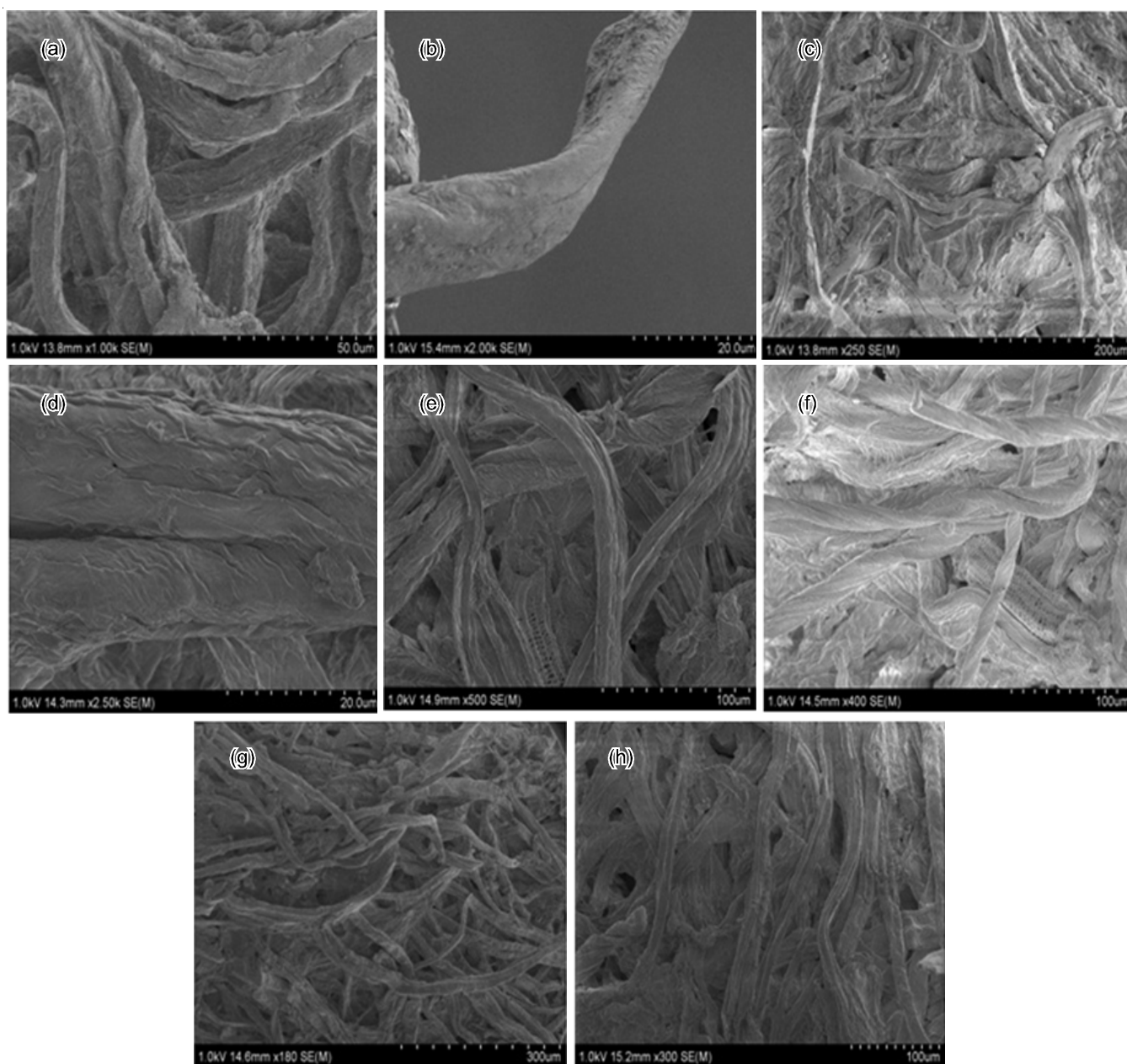


Fig. 4. SEM micrographs for cellulose prepared from (a,b) hemp, (c,d) pineapple leaf, (e,f) corn cob, (g,h) jackfruit peel

TABLE-5
ZONE OF INHIBITION OF DIFFERENT
FUNGI'S IN 1000, 750, 500 $\mu\text{g/mL}$

Organisms	Zone of inhibition (mm)			Antibiotic (1 mg/mL)
	1000 $\mu\text{g/mL}$	750 $\mu\text{g/mL}$	500 $\mu\text{g/mL}$	
<i>Trichoderma viride</i>	8	7	7	7
<i>Rhizopus stolonifer</i>	9	7	7	7
<i>Candida albicans</i>	10	8	8	12
<i>Aspergillus niger</i>	12	7	7	7
<i>Dermatophyte</i>	9	8	7	17

from these sources are investigated. The cellulose isolated from hemp shows more yield with comparatively promising physico-chemical properties. The cellulose isolated from hemp showed anti-microbial activity against *Bacillus subtilis* and *Dermatophyte*. This study demonstrated that the successful isolation

of cellulose from the renewable sources have high economical value with potential applications in biomedical fields

ACKNOWLEDGEMENTS

The authors acknowledge Dr. Amirthavalli Raghupathy Memorial Fund for providing the financial support. Thanks to The Principal, Presidency College (Autonomous), Chennai, Tamilnadu for providing access to DST-FIST Laboratory facility and also Dr. R. Baskar, SAIF, IIT Madras, Chennai, India.

CONFLICT OF INTEREST

The authors declare that there is no conflict of interests regarding the publication of this article.

REFERENCES

- C.M. Altaner, L.H. Thomas, A.N. Fernandes and M.C. Jarvis, *Biomacromolecules*, **15**, 791 (2014); <https://doi.org/10.1021/bm401616n>
- S.H. Cho, P. Purushotham, C. Fang, C. Maranas, S.M. Díaz-Moreno, V. Bulone, J. Zimmer, M. Kumar and B.T. Nixon, *Plant Physiol.*, **175**, 146 (2017); <https://doi.org/10.1104/pp.17.00619>
- V.V. Revin, E.V. Liyas'kina, N.B. Sapunova and A. O. Bogatyreva, *Microbiology*, **89**, 86 (2020); <https://doi.org/10.1134/S0026261720010130>
- A. Kumar, T. Jyske and M. Petric, *Adv. Sustain. Syst.*, **5**, 2000251 (2021); <https://doi.org/10.1002/advsu.202000251>
- K. Buzala, P. Przybysz, J. Rosicka-Kaczmarek and H. Kalinowska, *Cellulose*, **22**, 2737 (2015); <https://doi.org/10.1007/s10570-015-0644-9>
- G.A. Morris and S.E. Harding, Eds.: G.C.K. Roberts, *Hydrodynamic Modeling of Carbohydrate Polymers*. In: *Encyclopedia of Biophysics*. Springer, Berlin, Heidelberg (2013).
- J.T. McNamara, J.L.W. Morgan and J. Zimmer, *Annu. Rev. Biochem.*, **84**, 895 (2015); <https://doi.org/10.1146/annurev-biochem-060614-033930>
- A. Salama, *Int. J. Biol. Macromol.*, **127**, 606 (2019); <https://doi.org/10.1016/j.ijbiomac.2019.01.130>
- R.K. Singh and A.K. Singh, *Waste Biomass Valoriz.*, **4**, 129 (2013); <https://doi.org/10.1007/s12649-012-9123-9>
- M. Sasikala and M.J. Umapathy, *New J. Chem.*, **42**, 19979 (2018); <https://doi.org/10.1039/C8NJ02973C>
- A. Shalini, P. Paulraj, K. Pandian, G. Anbalagan and V. Jaisankar, *Surf. Interfaces*, **17**, 100386 (2019); <https://doi.org/10.1016/j.surf.2019.100386>
- C. Trilokesh and K.B. Uppuluri, *Sci. Rep.*, **9**, 16709 (2019); <https://doi.org/10.1038/s41598-019-53412-x>
- S. Mueller, C. Weder and E.J. Foster, *RSC Adv.*, **4**, 907 (2019); <https://doi.org/10.1039/C3RA46390G>
- L. Ravindran, S. M.S and S. Thomas, *Int. J. Biol. Macromol.*, **131**, 858 (2019); <https://doi.org/10.1016/j.ijbiomac.2019.03.134>
- A.A. Benhamou, Z. Kassab, A. Boussetta, M.H. Salim, E.-H. Ablouh, M. Nadifiyine, A. El Kacem Qaiss, A. Moubarik and M. El Achaby, *Int. J. Biol. Macromol.*, **203**, 302 (2022); <https://doi.org/10.1016/j.ijbiomac.2022.01.163>
- L.Y. Ng, T.J. Wong, C.Y. Ng and C.K.M. Amelia, *Arab. J. Chem.*, **14**, 103339 (2021); <https://doi.org/10.1016/j.arabjc.2021.103339>
- N. Stevulova, J. Cigasova, A. Estokova, E. Terpakova, A. Geffert, F. Kacik, E. Singovszka and M. Holub, *Materials*, **7**, 8131 (2014); <https://doi.org/10.3390/ma7128131>
- B.C. Okeke and S.K.C. Obi, *Bioresour. Technol.*, **47**, 283 (1994); [https://doi.org/10.1016/0960-8524\(94\)90192-9](https://doi.org/10.1016/0960-8524(94)90192-9)
- N. Shanugam, R.D. Nagarkar and K. Manisha, *Indian J. Nat. Prod. Resour.*, **6**, 42 (2015).
- N. Stevulova, J. Cigasova, A. Estokova, E. Terpakova, A. Geffert, F. Kacik, E. Singovszka and M. Holub, *Materials*, **7**, 8131 (2014); <https://doi.org/10.3390/ma7128131>
- R.M. Dos Santos, W.P.F. Neto, H.A. Silvério, D.F. Martins, N. Dantas and D. Pasquini, *Ind. Crops Prod.*, **50**, 707 (2013); <https://doi.org/10.1016/j.indcrop.2013.08.049>
- S. Suesat and P. Suwanruji, *Adv. Mater. Res.*, **332-334**, 1781 (2011); <https://doi.org/10.4028/www.scientific.net/AMR.332-334.1781>
- I.M. Fareez, N.A. Ibrahim, W.M.H. Wan Yaacob, N.A. Mamat Razali, A.H. Jasni and F. Abdul Aziz, *Cellulose*, **25**, 4407 (2018); <https://doi.org/10.1007/s10570-018-1878-0>
- F. Luzi, E. Fortunati, D. Puglia, M. Lavorgna, C. Santulli, J.M. Kenny and L. Torre, *Ind. Crops Prod.*, **56**, 175 (2014); <https://doi.org/10.1016/j.indcrop.2014.03.006>
- S.A. Ahmed, A.R. Kazim and H.M. Hassan, *World J. Exp. Biosci.*, **20**, 120 (2017).
- M.C.I. Mohd Amin, N. Ahmad, N. Halib and I. Ahmad, *Carbohydr. Polym.*, **88**, 465 (2012); <https://doi.org/10.1016/j.carbpol.2011.12.022>
- E. Arrebola, V.J. Carrión, J.A. Gutiérrez-Barranquero, A. Pérez-García, P. Rodríguez-Palenzuela, F.M. Cazorla and A. Vicente, *FEMS Microb. Ecol.*, **91**, 5071 (2015); <https://doi.org/10.1093/femsec/fiv071>
- R. Auta, G. Adamus, M. Kwiecien, I. Radecka and P. Hooley, *African J. Biotechnol.*, **16**, 470 (2017).
- H.M.C. Azeredo, H. Barud, R.S. Farinas, V.M. Vasconcellos and A.M. Claro, *Front. Sustain. Food Syst.*, **3**, 7 (2019); <https://doi.org/10.3389/fsufs.2019.00007>
- C. Babac, T. Kutsal and E. Piskin, *Int. J. Natural Eng. Sci.*, **3**, 19 (2009).
- S. Bae and M. Shoda, *Biotechnol. Prog.*, **20**, 1366 (2004); <https://doi.org/10.1021/bp0498490>
- H.S. Barud, T. Regiani, R.F. Marques, W.R. Lustrí, Y. Messaddeq and S.J. Ribeiro, *J. Nanomater.*, **2011**, 721631 (2011); <https://doi.org/10.1155/2011/721631>
- A. Bauer, W. Kirby, J. Sherris and M. Turck, *Am. J. Clin. Pathol.*, **45(4-ts)**, 493 (1966); <https://doi.org/10.1093/ajcp/45.4-ts.493>
- W. Czaja, A. Krystynowicz, M. Kawecki, K. Wysota, J. Glik, S. Sakiel, P. Wróblewski, M. Nowak and S. Bielecki, in Eds.: R.M. Brown and I.M. Saxena, *Biomedical Applications of Microbial Cellulose in Burn Wound Recovery*, In: *Cellulose: Molecular and Structural Biology*. Springer (2007); https://doi.org/10.1007/978-1-4020-5380-1_17
- Y.J. Bomble, C.Y. Lin, A. Amore, E.K. Holwerda, P.N. Ciesielski, B.S. Donohoe, H. Wei, P.R. Chawla, I.B. Bajaj, S.A. Survase and R.S. Singhal, *Food Technol. Biotechnol.*, **47**, 107 (2009).
- Y.J. Bomble, C.Y. Lin, A. Amore, H. Wei, E.K. Holwerda, P.N. Ciesielski, B.S. Donohoe, S.R. Decker, L.R. Lynd and M.E. Himmel, *Curr. Opin. Chem. Biol.*, **41**, 61 (2017); <https://doi.org/10.1016/j.cbpa.2017.10.013>
- Y.J. Choi, Y. Ahn, M.S. Kang, H.K. Jun, I.S. Kim and S.H. Moon, *J. Chem. Technol. Biotechnol.*, **79**, 79 (2004); <https://doi.org/10.1002/jctb.942>
- A.F.S. Costa, F.C.G. Almeida, G.M. Vinhas and L.A. Surubbo, *Front. Microbiol.*, **8**, 2027 (2017); <https://doi.org/10.3389/fmicb.2017.02027>
- D. Pérez-Mendoza, A. Felipe, M.D. Ferreira, J. Sanjuán and M.T. Gallegos, *Front. Microbiol.*, **10**, 746 (2019); <https://doi.org/10.3389/fmicb.2019.00746>
- G.A. Farias, A. Olmedilla and M.T. Gallegos, *Microb. Biotechnol.*, **12**, 688 (2019); <https://doi.org/10.1111/1751-7915.13385>
- J.F. Godinho, F.V. Berti, D. Müller, C.R. Rambo and L.M. Porto, *Cellulose*, **23**, 545 (2016); <https://doi.org/10.1007/s10570-015-0844-3>
- M. Iguchi, S. Yamanaka and A. Budhiono, *J. Mater. Sci.*, **35**, 261 (2000); <https://doi.org/10.1023/A:1004775229149>
- R. Kumar, G. Mago, V. Balan and C.E. Wyman, *Bioresour. Technol.*, **100**, 3948 (2009); <https://doi.org/10.1016/j.biortech.2009.01.075>